Theoretical Analysis of Gradient Detection by Growth Cones

Geoffrey J. Goodhill,[1] Jeffrey S. Urbach[2]

[1] Georgetown Institute for Cognitive and Computational Sciences, Georgetown University Medical Center, 3970 Reservoir Road, Washington, DC 20007

[2] Department of Physics, Georgetown University, 37th and O Streets, Washington, DC 20057

Received 10 February 1999; accepted 5 April 1999

ABSTRACT: Gradients of diffusible and substrate-bound molecules play an important role in guiding axons to appropriate targets in the developing nervous system. Although some of the molecules involved have recently been identified, little is known about the physical mechanisms by which growth cones sense gradients. This article applies the seminal Berg and Purcell (1977) model of gradient sensing to this problem. The model provides estimates for the statistical fluctuations in the measurement of concentration by a small sensing device. By assuming that gradient detection consists of the comparison of concentrations at two spatially or temporally separated points, the model therefore provides an estimate for the steepness of gradient that can be detected as a function of physiological parameters. The model makes the following specific predictions. (a) It is more likely that growth cones use a spatial rather than temporal sensing strategy. (b) Growth cone sensitivity increases with the concentration of ligand, the speed of ligand diffusion, the size of the growth cone, and the time over which it averages the gradient signal. (c) The minimum detectable gradient steepness for growth cones is roughly in the range 1–10%. (d) This value varies depending on whether a bound or freely diffusing ligand is being sensed, and on whether the sensing occurs in three or two dimensions. The model also makes predictions concerning the role of filopodia in gradient detection. J Neurobiol 41: 230–241, 1999

Keywords: **growth cone; chemotropism; gradients; axon guidance; theoretical model**

For the brain to function correctly, its neurons must be connected correctly. Understanding how axons are guided to appropriate targets is thus crucially important for understanding how both normal and abnormal brains develop. Recent experimental work has made major advances in uncovering the mechanisms involved in axon guidance (Keynes and Cook, 1995; Goodman, 1996; Tessier-Lavigne and Goodman, 1996), and has identified receptor/ligand pairs such as netrin/DCC (Kennedy et al., 1994; Serafini et al., 1994; Colamarino and Tessier-Lavigne, 1995; Keino-Masu et al., 1996; Serafini et al., 1996; Deiner et al., 1997; Richards et al., 1997) and the ephrin/Eph family (Cheng et al., 1995; Drescher et al., 1995; Gale et al., 1996; Gao et al., 1996; reviewed in Flanagan and Vanderhaegen, 1998; O'Leary et al., 1999) as playing crucial roles in guidance in multiple systems. A common theme in much of this work, particularly for the receptors and ligands mentioned above, is guidance by concentration gradients (reviewed in Tessier-Lavigne and Placzek, 1991). Ligand gradients can be set up by diffusion (Lumsden and Davies, 1983, 1986; Heffner et al., 1988; Tessier-Lavigne et al., 1988; Placzek et al., 1990; Pini, 1993; Kennedy and Tessier-Lavigne, 1995; Keynes et al., 1997), by graded expression on cell membranes (see Eph/ephrin refer-

Correspondence to: G. J. Goodhill

Contract grant sponsor: DOD; contract grant number: DAMD17-93-V-3018

 CCC 0022-3034/99/020230-12

ences above), or by binding of diffusible factors to a substrate (e.g., Stoekli et al., 1997). These gradients can exist in a three-dimensional volume, as in the guidance of commissural axons to the floor plate, or on a two-dimensional surface, as may be the case for guidance of retinal ganglion cell axons across the tectum. Axons move up or down these gradients until they reach their targets, or until other guidance cues take over or provoke a change in the way the axon interprets the gradient signal (e.g., Song et al., 1997; Ming et al., 1997; Shirasaki et al., 1998).

What are the physical mechanisms by which axons sense such gradients? To address this, it is useful to draw an analogy with gradient sensing by leukocytes and bacteria (Tessier-Lavigne and Placzek, 1991). Chemotaxis in these latter two systems has been well-characterized experimentally (leukocytes: Zigmond, 1977, 1981; Devreotes and Zigmond, 1988; Lauffenburger et al., 1988; bacteria: Macnab and Koshland, 1972; Dahlquist et al., 1972; Adler, 1975; Berg, 1975; Manson, 1992; Eisenbach, 1996), and many physical models and quantitative analyses have been developed to account for these data (Berg and Purcell, 1977; Segel, 1977; Alt, 1980; Lauffenburger, 1982; DeLisi et al., 1982; DeLisi and Marchetti, 1983; Tranquillo and Lauffenburger 1986, 1987; Ford, 1992). These models provide physical limits on what can be achieved by particular mechanisms for gradient detection. Our aim is to derive a similar understanding of axonal chemotaxis in the developing nervous system. Previously, we considered how gradient shape constrains axon guidance given crude assumptions about the gradient sensing mechanism (Goodhill, 1997, 1998). Here, we consider in detail the mechanism itself, by applying the seminal Berg and Purcell (1977) model of gradient sensing to growth cones. Although subsequent models have developed the Berg and Purcell theory further, they are substantially more complicated mathematically, and also depend on numerous additional parameters which have not been determined in the context of axon guidance. The Berg and Purcell model provides theoretical predictions of experimentally measurable quantities such as the minimum detectable gradient steepness, the maximum distance over which an axon could be guided by a single gradient, how these quantities vary with growth cone size, the time over which it averages a gradient signal, the number of receptors, and the diffusion rate of the ligand. It also sheds light on whether axons use a spatial or temporal gradient sensing mechanism, the role that filopodia could play in gradient sensing, and the differences between gradient detection for a two- compared to three-dimensional substrate, and between a diffusible compared to substrate-bound factor.

MATERIALS AND METHODS

Berg and Purcell (1977) analyzed the physical constraints underlying concentration measurement by a small sensing device that relies on a limited number of receptors. This analysis can be applied straightforwardly to gradient measurement by assuming that gradient detection is simply the comparison of two different concentrations. Berg and Purcell calculated the statistical noise that arises from variations in the number of receptors bound at any instant, caused by the random movement of ligand molecules near the sensing device. Random fluctuations in the intracellular events that transduce the difference in binding signal are not considered. They calculate the root mean square fluctuation in the estimate of concentration in some small volume ΔC_{noise}, giving the fractional error $\Delta C_{\text{noise}}/C$. The fractional root mean square error in the measurement of a concentration difference between two spatially or temporally separated points is then $\sqrt{2}\Delta C_{\text{noise}}/C$, assuming that ΔC_{noise} and C are about the same at both points. For a true gradient to be detected, it must be steep enough so that the actual concentration difference between the two sides of the cell, ΔC_{grad}, is such that

$$\Delta C_{\text{grad}}/C > \sqrt{2}\Delta C_{\text{noise}}/C$$

Berg and Purcell calculated $\Delta C_{\text{noise}}/C$, making a number of simplifying assumptions: The sensing device is spherical, receptors are uniformly distributed, receptors are perfectly absorbing (the ligand is internalized), the receptor–ligand reaction is purely bimolecular, the receptor–ligand reaction is diffusion limited, fluctuations are averaged over a time much greater than that required for receptor binding to come to equilibrium, rate constants are occupancy independent, and ligand concentration is not significantly depleted by receptor binding. The validity of these assumptions for growth cones is considered in the Discussion. It follows from these that the fluctuations in the number of bound receptors follow the instantaneous thermal fluctuations in the number of ligand molecules in the vicinity of the cell. Berg and Purcell imagined a spherical cell of radius a, which we will identify with a growth cone of radius a, immersed in a large bath containing a low concentration of a ligand. The cell has N receptors for the ligand. The diffusive current J to the cell—that is, the rate at which molecules are absorbed by the cell and become available for concentration measurement (also called the flux)—is

$$J = 4\pi DCa$$

where D is the diffusion constant of the ligand and C is the (constant) concentration far from the cell. When ligand molecules can be internalized only through a finite number N of receptors of radius s, assumed very much smaller than a, and roughly uniformly distributed over the cell, this formula becomes

$$J = 4\pi DCa \frac{Ns}{Ns + \pi a}$$

Berg and Purcell performed several increasingly sophisticated calculations for $\Delta C_{\text{noise}}/C$ in this case, the simplest of which is as follows. Roughly, $\Delta C_{\text{noise}}/C = 1/\sqrt{m}$, where m is the number of molecules in the vicinity of the cell. This equals $1/\sqrt{VC}$, where C is the ligand concentration and V is the volume around the cell, roughly equal to a^3. However, this is for an instantaneous measurement. If the concentration is instead averaged over M measurements suitably spaced in time, the fractional error is reduced by roughly $1/\sqrt{M}$. "Suitably spaced" means allowing sufficient time for a molecule that is counted in one measurement to diffuse away before being counted again: about a^2/D. Thus, if the total averaging time available is T, then in three dimensions

$$\frac{\Delta C_{\text{noise}}}{C} = \frac{1}{\sqrt{aDTC}} \quad (1)$$

In two dimensions, the equivalent formula is

$$\frac{\Delta C_{\text{noise}}}{C} = \frac{1}{\sqrt{DTC}} \quad (2)$$

where C is now a concentration of ligand molecules per unit area rather than per unit volume. Note that now the formula does not depend on a, the size of the growth cone. Intuitively, as the growth cone gets larger there are two competing effects: More ligand molecules are encountered, but they each take longer to diffuse away, and thus fewer independent measurements can be made in a given time T. In the three-dimensional case, the former effect wins over the latter, but in two dimensions they exactly cancel.

Using more sophisticated methods, Berg and Purcell also calculated $\Delta C/C$ for a measuring instrument which relies on the statistics of binding to a finite number of receptors to assess concentration. In the three-dimensional case, this has the form

$$\frac{\Delta C_{\text{noise}}}{C} = \sqrt{\frac{1}{2\pi TDa \dfrac{Ns}{Ns + \pi a} \dfrac{CC_{1/2}}{C + C_{1/2}}}} \quad (3)$$

where $C_{1/2}$ is the concentration at which half the receptors are bound, i.e., the dissociation constant K_{D} (measured in units of molecules per volume). Note that the fractional uncertainty given by Equation (3) tends to a constant as C increases above $C_{1/2}$: Intuitively, there are two competing tendencies. On the one hand, there are more ligand molecules available for making a comparison, and the uncertainty goes down. On the other hand, an increasingly high proportion of receptors will be bound, and the uncertainty goes up. In Equation (3), these two tendencies exactly cancel, and the uncertainty tends to a constant for large C. Parameters and their meaning are given in Table 1.

Table 1 Parameters and Their Meanings

Parameter	Meaning
D	Diffusion constant
C	Ligand concentration at the growth cone
$C_{1/2}$	Ligand concentration at which half the receptors are bound (k_{D}).
$C_{\max}$	Maximum ligand concentration at which a gradient is detectable
ΔC_{noise}	RMS fluctuation in concentration in a small volume
ΔC_{grad}	Concentration difference across a small volume due to the gradient
J	Flux of molecules impinging on a small volume
a	Radius of a growth cone
N	Number of receptors on a growth cone
s	Effective receptor radius
T	Time over which a growth cone averages concentration fluctuations

For parameter values used to derive numerical results, see text.

RESULTS

Minimum Detectable Gradient

To evaluate a model for the mechanisms of gradient detection by growth cones, some quantitative predictions of the model must be compared with experiment. The most obvious such prediction is the minimum change in concentration that a growth cone can detect across its spatial extent. Consider a growth cone sampling a spherical volume of radius 10 μm, in a ligand concentration of 1 nM (roughly the value of the dissociation constant for many receptor–ligand pairs implicated in axon guidance (see references cited in Goodhill and Baier, 1998)). This volume contains about 2500 molecules, and the fractional error in an instantaneous measurement of the gradient in this case is therefore about $1/\sqrt{2500}$, or 2%. However, growth cones take a time of the order of a minute to show a response to a gradient signal (Zheng et al., 1996), which suggests they may be averaging concentration measurements over a time T of order

100 s. For a freely diffusing molecule the size of netrin in a liquid, the diffusion constant $D \approx 10^{-6}$ cm^2/s, whereas *in vivo*, $D \approx 10^{-7}$ cm^2/s (reviewed in Goodhill, 1997). For proteins bound to cell membranes, experimental values have been obtained in the range $D = 10^{-8}$ cm^2/s to $D = 10^{-11}$ cm^2/s (Wiegel, 1983); for instance, Poo (1982) found a value of $D = 2.6 \times 10^{-9}$ cm^2/s for acetylcholine (ACh) receptors diffusing over the surface of embryonic muscle cells. Therefore, taking $D \approx 10^{-9}$ cm^2/s for membrane-bound ligands yields values from Equation (1) in the (three-dimensional) liquid, *in vivo*, and membrane-bound cases of 0.5%, 1%, and 10%, respectively. The model therefore predicts that shallower gradients of a diffusible factor are detectable than gradients of a bound factor.

In two dimensions rather than three, Equation (2) is applicable rather than Equation (1). Ligand concentration densities have not been measured in relevant two-dimensional cases—for instance, for ephrin molecules in the tectum. A summary of the concentration density on cell membranes of a large number of enzymes and proteins (McCloskey and Poo, 1986) suggests that generally these lie in the range 10^9 to 10^{11} molecules/cm^2. Assuming a diffusion constant for bound ligands in the range 10^{-9} to 10^{-11} cm^2/s gives values for the minimum detectable gradient of about 1–10%. Thus, the model predicts that the minimum detectable gradient in two-dimensional cases is similar to or slightly higher than the minimum detectable gradient in three-dimensional cases. It is remarkable that despite the different combination of parameter values that give the minimum detectable gradient in the two- and three-dimensional cases, the numerical predictions are similar.

Receptor numbers have been measured in the case of, for example, neurotrophin receptors on embryonic sensory neurons (not growth cones themselves), yielding numbers between a few hundred and about 50,000 (reviewed in Meakin and Shooter, 1992). If $N = 10{,}000$, $s = 50$ angstroms, and $K_D = 1$ n*M*, this yields values for the fractional gradient error given by Equation (3) in the three-dimensional case very similar to those for the rough calculation above (note that the gradient error varies only as the square root of most of the parameters, so that a variation of an order of magnitude in a parameter yields a change of only a factor of three in the gradient error). $N = 10{,}000$ is the number of receptors for which the sphere collects half the available flux, even though only a tiny fraction of the surface area is covered by receptors (Berg and Purcell, 1977). If $N = 100$, the minimum detectable gradient would be 10 times greater.

Further insight can be derived by examining graphically the dependence of the minimum detectable gradient on experimentally relevant parameters in the three dimensional case. Figure 1(A) shows the gradient sensitivity calculated from Equation (3) as a function of averaging time for four different values of the total number of receptors. (Or, conversely, the averaging time necessary to detect a particular fractional concentration change.) As described by Berg and Purcell, a relatively small density of receptors effectively covers a surface, as can be seen from the small difference between the sensitivities of growth cones with 10,000 and 100,000 receptors. Increasing the averaging time, however, always results in significantly increased sensitivity. Observed turning times range from about 1 min in the presence of a fractional gradient of about 10% *in vitro* (Zheng et al., 1996), to over 1 h in an unknown gradient *in vivo* (Myers and Bastiani, 1993). The plots demonstrate that the gradient *in vivo* may be considerably weaker than that necessary to generate a turning response on the short time scale of the *in vitro* experiments. The diffusion coefficient appears in Equation (3) only in combination with the averaging time, so a plot of sensitivity as a function of diffusion coefficient for fixed averaging time would look identical.

Figure 1(B) shows how the gradient sensitivity depends on the number of receptors. For large receptor density, the sensitivity is almost independent of receptor number, as described above. The saturation sets in when $Ns \approx \pi a$, which is about $N = 10{,}000$ for the parameters used in Figure 1(B). The sensitivity decreases rapidly as N is decreased below that value, because ligand molecules typically will diffuse for a long time before encountering a receptor. The dependence of the sensitivity on the average ligand concentration is shown in Figure 1(C) for four different values of the averaging time. In all cases, the dissociation constant is 1 n*M*. The sensitivity decreases rapidly below the dissociation constant and saturates above it. This is a consequence of the exact cancellation of the effects of the number of ligand molecules and the proportion of receptors bound. The dependence of the sensitivity on the growth cone size is shown in Figure 1(D) for both constant receptor number and constant receptor density. Note that large increases in growth cone size offer little improvement unless they are accompanied by an increase in the number of receptors.

Spatial versus Temporal Sensing Mechanisms

In a spatial sensing mechanism, a concentration comparison is made between the two sides of the sensing

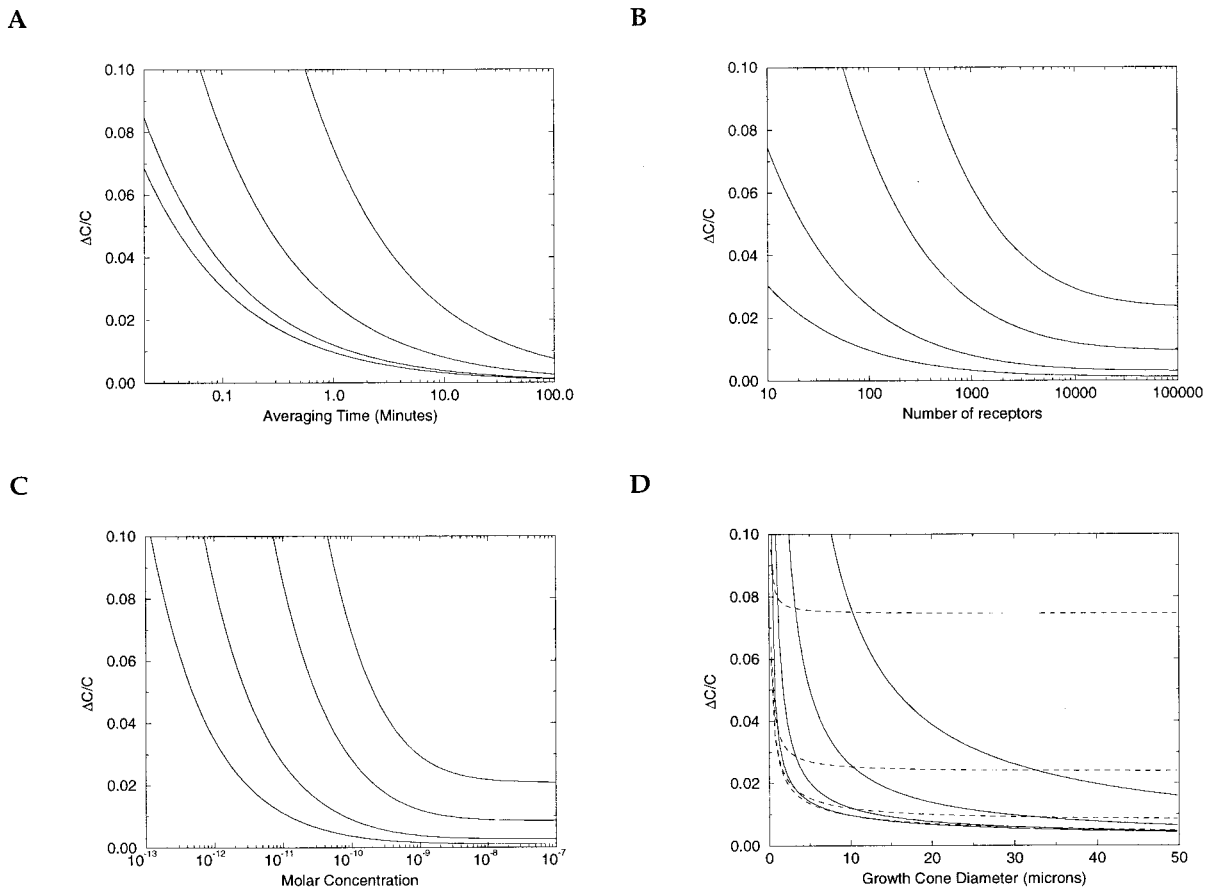

Figure 1 Fractional uncertainty in concentration measurement calculated from Equation (3) as a function of several parameters. (A) Time used to average information about receptor binding. The four lines are for different values of the total number of receptors on the growth cone. From left to right: $N = 100{,}000$, 10,000, 1000, and 100. Parameters: Growth cone diameter $a = 10$ μm, diffusion coefficient $D = 10^{-7}$ cm^2/s, receptor diameter $s = 50$ angstroms, average concentration and $K_D = 1$ n*M*. (B) Total number of receptors on the growth cone. The four lines are for different values of the averaging time. From left to right: $T = 1$ h, 10 min, 1 min, and 10 s [other parameters as in (A)]. (C) Mean ligand concentration. The four lines are for different values of the averaging time. (Left to right) $T = 1$ h, 10 min, 1 min, and 10 s. Parameters: as in (A) with $n = 10{,}000$. (D) Growth cone size for constant receptor number (dashed lines) and constant receptor density (solid lines). Parameters as before with an averaging time of 1 min. Dashed lines from bottom to top: $n = 100{,}000$, 10,000, 1000, and 100. Solid lines from bottom to top: 300, 30, 3 and 0.3 receptors/μm^2 (30 gives about 10,000 on a 10-μm-diameter growth cone).

device. In a temporal sensing mechanism, the sensing device measures the overall receptor occupancy at one position, moves to a new position, and then measures overall receptor occupancy again. It is generally believed that leukocytes use a spatial mechanism (Zigmond, 1974), whereas bacteria use a temporal mechanism (Macnab and Koshland, 1972; Adler, 1975; Berg, 1975). Under the assumptions of the Berg and Purcell model, a spatial sensing mechanism is clearly more efficient than a temporal mechanism for growth cones since they move so slowly. To compare the concentrations in two regions that are further apart than the width of the growth cone would require waiting a period of several minutes for the growth cone to move that far. As the calculations above show, a gradient of just a few percent can be detected in far less time using a spatial mechanism. (Note that one advantage of a temporal mechanism is that the concentration can be measured over the whole growth cone, rather than just the smaller areas of each half of the growth cone as for a spatial mechanism. However, this degrades the sensitivity of the spatial mechanism by only a factor of $\sqrt{2}$, which is insignificantly small for the argument above.) Other problems with a tem-

poral mechanism in this case are that the growth cone would have to remember its previous concentration estimate for several minutes, and growth cone trajectories are smooth and not biased random walks as would be expected from a temporal mechanism (Ford, 1992). However, an interesting difference occurs for growth cones sensing a bound gradient. The lower diffusion constant means that the growth cone would have to wait about 10 times longer to derive the same gradient information from a spatial mechanism. Since 1000 s is substantially longer than the time observed experimentally for growth cones to begin turning in a particular direction, in this case the model predicts that a temporal mechanism might be more favorable since the growth cone can move itself to a position to sample an independent population of ligand molecules about as fast as the molecules themselves move by diffusion. If this is true, axon trajectories would be expected to be less smooth in substrate-bound gradients than diffusible gradients; however there is presently no evidence for this.

Maximum Guidance Distance

What is the optimal gradient shape under the Berg and Purcell model for guiding an axon over the maximum possible distance, and what is this maximum distance? The optimal gradient has a percent concentration change across each growth cone diameter equal to the minimum required for gradient detection. Setting $\frac{a}{C}\frac{dC}{dx}$ equal to Equation (3) and integrating gives

$$x = -a\sqrt{\pi TDaC_{1/2}\frac{Ns}{Ns+\pi a}} \times \log\left[2\left(\sqrt{C^2 + CC_{1/2}} + C + C_{1/2}/2\right)\right] + B \quad (4)$$

where B is an arbitrary constant of integration. The value of this constant can be set by imposing the condition that $C = C_{\max}$ when $x = 0$, where $C_{\max}$ is a maximum allowable concentration. This assumption is motivated by experimental data both from leukocytes and the experiments of Ming et al. (1997), that, owing to factors not considered in the Berg and Purcell model, gradient detection is not possible above a certain high concentration limit of about 10 to 100 times $C_{1/2}$. This function is shown in Figure 2. Note that it is convex: The lower the concentration, the steeper the gradient that is required to be detectable. Thus, a prediction of the model is that a convex shape would be required for effective guidance over distances of several millimeters.

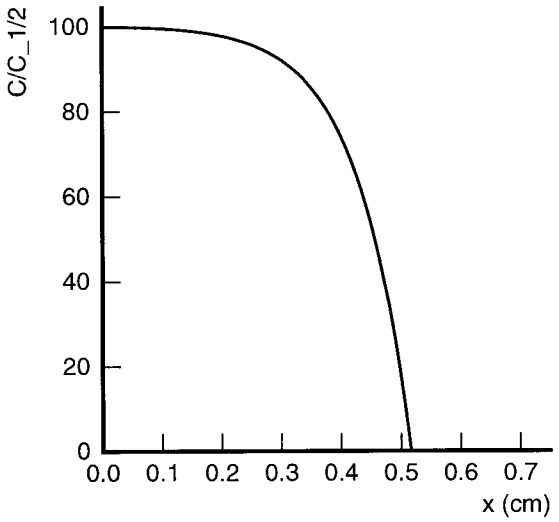

Figure 2 Optimally shaped gradient according to the Berg and Purcell model (a plot of $C/C_{1/2}$ against distance). The lower the concentration, the steeper the gradient required for detection.

The maximum guidance distance $x_{\max}$ is found from Equation (4) by setting $C = 0$. This gives

$$x_{\max} = a\sqrt{\pi TDaC_{1/2}\frac{Ns}{Ns+\pi a}} \times \log\left[\frac{\sqrt{C_{\max}^2 + C_{\max}C_{1/2}} + C_{\max} + C_{1/2}/2}{C_{1/2}/2}\right]$$

If $C_{\max} \gg C_{1/2}$, $x_{\max}$ can be rewritten approximately as

$$x_{\max} = a\sqrt{\pi TDaC_{1/2}\frac{Ns}{Ns+\pi a}}\log\left(4C_{\max}/C_{1/2}\right)$$

Both the log term and the term inside the square root are dimensionless, so $x_{\max}$ has dimensions of length as required. Substituting in our previous estimates for the parameters and setting $C_{\max} = 100C_{1/2}$ yields an order of magnitude for $x_{\max}$ of 1 cm. This fits well with previous estimates based on a much cruder model of the gradient sensing process (Goodhill and Baier, 1998; Goodhill, 1998), but now makes specific predictions for how this varies with parameters such as T, D, and N.

Effectiveness of Filopodia for Gradient Sensing

The above analysis assumes the growth cone is spherical, and does not take into account the effect of

filopodia (reviewed in Rehder and Kater, 1996). It is possible that an individual filopodium could use a temporal gradient sensing mechanism, comparing the concentrations either between early and late parts of its trajectory from the growth cone, or between two points equally distant from the growth cone separated by a small angle. However, on the scale of the whole growth cone this is equivalent to a spatial sensing mechanism (this has been called "pseudospatial" sensing in the context of leukocytes) (Tranquillo, 1990). In addition, the movement of the filopodia moves the receptors they express, and so in principle could increase the rate at which receptors encounter ligand molecules. It would take about 1 min for a receptor to move 10 μm by being carried along by an extending filopodium moving at 0.2 μm/s (Tanaka and Sabry, 1995). However, in this time it would also be expected to move a distance of about $\sqrt{Dt} \approx 10$ μm by diffusion through the membrane. Thus, the filopodia motion seems to confer no particular advantage for gradient sensing compared to a sphere, at least in terms of increasing the rate at which receptors come into contact with ligand molecules. However, the filopodia structure does allow the growth cone to increase its effective sensing radius. An alternative approach is to define an effective diffusion constant D_f for filopodia equal to velocity $\times$ width: this has appropriate units for a diffusion constant and expresses the notion of measuring the area explored per unit time. For a filopodial width of 0.5 μm (Tanaka and Sabry, 1995) $D_f \approx 10^{-9}$ cm^2/s, which is of the same order as the diffusion constant of receptors in the membrane.

However, growth cones display smooth trajectories, unlike the biased random walks of leukocytes and bacteria. To explore this issue further we combined the Berg and Purcell model with a more detailed model of filopodial dynamics. Zheng et al. (1996) demonstrated that the distribution of filopodia on the growth cone becomes asymmetric only minutes after the application of a chemotropic factor (glutamate in this case), while the turning response of the growing neurite was only measurable after about 30 min. Furthermore, the turning response was strongly inhibited when the filopodia were eliminated by treatment with cytochalasin B. These results suggest that the filopodia are at least partly responsible for gradient detection, and that the distribution of filopodia on the growth cone determines the direction of neurite extension. This might explain one of the fundamental differences between axon chemotaxis and the behavior observed in bacteria and leukocytes. In the absence of a gradient, the latter exhibit a random walk. The chemotaxis can be understood as a biased random walk, and significant turning is observed only when the system has moved distances large compared to the characteristic steps that make up the walk. Axons, by contrast, tend to grow in an approximately straight line, and seem to turn smoothly toward a sufficiently strong chemotropic source. If neurite turning is determined by averaging the stochastic response of a number of filopodia [about 15 in the experiment of Zheng et al. (1996)], in the absence of a bias (such as that due to a gradient), the average amount of turning will tend to be very small. In the presence of a gradient, the essentially stochastic nature of chemical sensing will be masked by the averaging of the filopodia, resulting in directed motion.

From the observations of Zheng et al. (1996), we consider 15 filopodia that have finite lifetimes, where each retraction is followed immediately by a new extension. We suppose that the growth cone tries to sprout new filopodia in the direction of the maximum concentration of the chemotropic factor, but that the accuracy of the determination of concentration is limited by the stochastic fluctuations. In our simulation, the direction of these is random, and the strength of the fluctuations is determined from Equation (3), extended to allow for nonspherical objects (Berg, 1993). Typical simulated trajectories with and without a chemotropic gradient are shown in Figure 3(A). For the simulations shown, we assumed 100 receptors/filopodium, a mean concentration at the growth cone of 1 μM [equal to the dissociation constant for glutamate binding to the NMDAR1 receptor (Hollmann and Heinemann, 1994) and the estimated concentration for maximum response from Zheng et al. (1996)] and that each filipodium is replaced every 3 min (i.e., a retraction/extension event occurs every 12 s). The trajectory in a strong gradient shows a clear turning toward the right (increasing factor concentration), while there is little deviation observed in the absence of a gradient. Experimental observations of a number of axons can be simulated by choosing different seeds for the random number generator. Figure 3(B) shows the turning angle of 30 simulated neurons after 30 min. Both the average turning angle and the standard deviation are similar to those observed by Zheng et al. (1996) at the glutamate concentrations where maximum response was observed. As described in Materials and Methods, the right-hand side of Equation (3) approaches a constant at high concentrations, so the simulations do not show the decrease in turning response at higher concentrations observed by Zheng et al. (1996). This issue is discussed further in the Discussion. The general behavior displayed in Figure 3

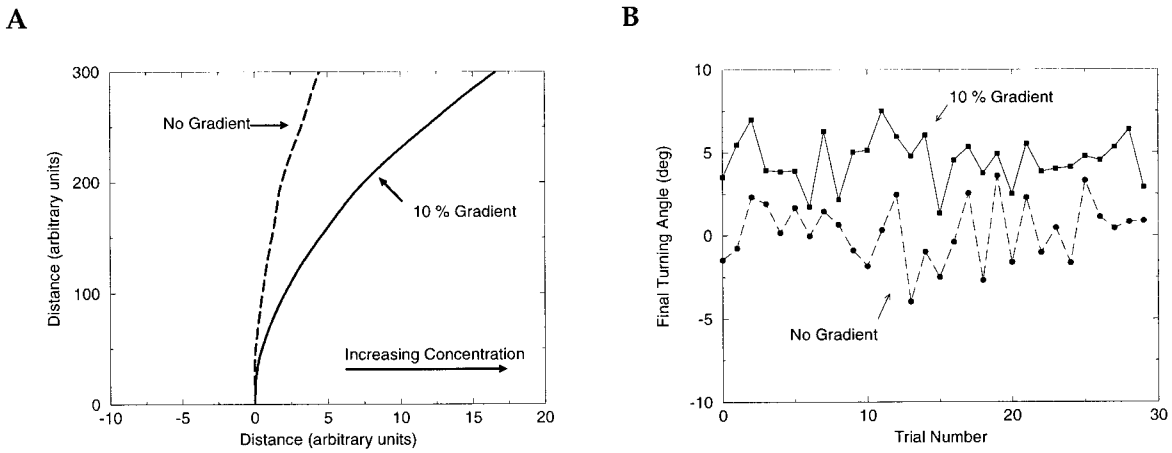

Figure 3 Results of model of growth cone gradient detection and turning mediated by filopodia. (A) Typical trajectories in the model for a growth cone in the presence and absence of a gradient that increases to the right. (B) Comparison of the response of a population of 30 growth cones to the case of no gradient and a 10% gradient. Each trial started from a different random initial condition (each set of points is joined by lines to make the two populations easier to distinguish). It can be seen that in a 10% gradient there is a robust turning response, but in the absence of a gradient there is no net turning.

is not very sensitive to the precise parameter values, and is a consequence of the assumptions about the dynamics.

DISCUSSION

For the Berg and Purcell model, the minimum gradient steepness that can be detected depends on the diffusion constant for the ligand, which depends on whether it is diffusing in liquid, through tissue, or within cell membranes. The limiting values in these three cases for a growth cone of radius 10 μm with 10,000 receptors moving in three dimensions are about 0.5%, 1%, and 10%, respectively, assuming that the local concentration is equal to $K_D = 1$ n*M*. These limiting values would be increased for larger growth cones, more receptors, a longer averaging time, and a higher local concentration. For sensing in two dimensions, the minimum detectable gradient steepness depends in a different way on the parameters, yet similar or slightly larger estimates emerge. The maximum guidance distance predicted by the model is about 1 cm. A simple analysis of the role of filopodia in gradient sensing suggests that they do not significantly increase the receptor–ligand encounter rate. A more detailed model, where the movement of each filopodium is assumed to be governed by the Berg and Purcell limits, reproduces recent data regarding the role of filopodia in growth cone turning.

Comparison with Experiment

There are few quantitative measurements of the size of the gradient a growth cone can detect. The most precise determinations in the case of diffusible factors have been made by Poo and colleagues (e.g., Lohof et al., 1992; Zheng et al., 1994; de la Torre et al., 1997). They found that growth cones could respond to a gradient of 5–10% across their width in liquid. However, the size of the smallest gradient required for detection was not determined. Even in the case of the lowest concentration (retinal growth cones responding to a gradient of netrin-1 (de la Torre et al., 1997), where $C \approx K_D \approx 1$ n*M*), the above predictions suggest that, assuming growth cones act as perfect measuring instruments, significantly shallower gradients should also be detectable in this case.

A clear example of two-dimensional sensing is the growth of axons on a substrate-bound gradient *in vitro*, as, for instance, in Baier and Bonhoeffer (1992), Halfter (1996), and Rosentreter et al. (1998). *In vivo*, a possible candidate for two-dimensional sensing is the growth of retinal ganglion cell axons over the surface of the tectum. Data from experiments with substrate bound gradients are difficult to interpret, however, since here only relative rather than absolute levels of ligand have been determined. Baier and Bonhoeffer (1992) estimated from their data that the minimum detectable gradient of tectal membrane density a retinal growth cone could detect across its width is 1%. However, by this they meant 1% of the max-

imum concentration at the high end of the gradient, whereas in the current article 1% means that the ratio of concentrations at the two sides of the growth cone is 1.01. Thus, 1% in the former sense translates into a percentage in the latter case that varies from large values at the low end of the gradient to small values at the high end of the gradient. However, in the upper part of the gradient the definitions give roughly similar results: moving from 50% to 51% of maximum concentration gives a percent change according to our definition of 2%, and moving from 99% to 100% of maximum concentration gives a percent change according to our definition of 1%. Baier and Bonhoeffer's estimate of 1% is thus very roughly consistent with the predictions made by the model. The gradients produced by Rosentreter et al. (1998) are more precisely controlled to be linear, but since a linear gradient has a constantly decreasing percentage change in concentration across the growth cone as one moves up the gradient, these data are again hard to interpret in terms of the model. For further discussion of the effect of gradient shape on sensing, see Goodhill and Baier (1998).

The calculations of Goodhill (1997, 1998) show that for a diffusible molecule released at a constant rate from a small target, the gradient across a 10-μm growth cone is $>2\%$ at all positions closer than 500 μm to the source, independent of the diffusion constant. Sensitivity also depends on the concentration, however, which depends on the rate of ligand production by the source. Consider the case of netrin released from the floor plate, diffusing dorsally through the spinal cord and establishing a gradient to guide commissural axons to the midline. If netrin diffuses freely through the tissue, the fractional change over 10 μm is at least 2%, but the overall concentration C is completely unknown. For the model of Goodhill (1997) $C \propto q$, the rate of production of netrin by the floor plate. For C to be 1 nM after 1 day at a distance of 500 μm would require a rate of production of about $q = 10^{-7}$ nM/s. If, however, some of the netrin binds to the substrate, gradient detection is now affected by the bound concentration, the free concentration, and the way in which the growth cone integrates these two types of information. A prediction of the model is that the bound gradient is virtually irrelevant compared to the free gradient. All that matters is the receptor–ligand encounter rate, which is set by the diffusion constant, and this is much higher for the fraction of ligand that is diffusible. In this scenario, the bound ligand gradient becomes important only if the relative amount of free ligand is very small. Bound netrin has been found in many places in the embryonic chick nervous system (MacLennan et al., 1997).

An analysis of the potential role of filopodial movement in gradient sensing suggests that this does not significantly improve gradient detection, since it does not enhance receptor–ligand encounter rates. This suggests a possible reason why growth cones slow down and adopt more complex morphologies at choice points (e.g., Mason and Wang, 1997): If these are points at which gradients are very shallow, slowing down may increase the averaging time for concentration measurement, which improves gradient measurement, and the altered morphology ensures that filopodia can sample more completely the local volume. Recently it has been shown that filopodia in *Xenopus* spinal neurons develop an asymmetry rather quickly in response to an applied glutamate gradient, showing an excess of filopodia on the high concentration side of the growth cone minutes after the appearance of the gradient (Zheng et al., 1996). While this asymmetry may serve to generate an asymmetric tension that helps orient the developing neuron, it has interesting implications for gradient sensing. By increasing the density of receptors on the high concentration side of the growth cone, the growth cone can in principle more precisely identify the direction of the maximum gradient. Experimentally, this dynamic refining of the guidance mechanism would show up as a surprisingly accurate targeting mechanism.

Limitations of the Model

Although the Berg and Purcell model is a relatively sophisticated model of gradient sensing, its assumptions are still restrictive. Growth cones are not spherical and their receptors are probably not uniformly distributed, although these particular assumptions may not be too important since only a small proportion of the surface need be covered by receptors to capture a large proportion of the flux. More restrictive are the assumptions about the nature of the reaction and the reaction rates. For the binding of nerve growth factor (NGF) to its high affinity receptor trkA, $t_{1/2}$ is about 10 min (Sutter et al., 1979; Meakin and Shooter, 1992), violating the assumption that many independent measurements of receptor occupancy can be made in $T \approx 100$ s. Sutter et al. (1979) measured rate constants for the binding of NGF to the high-affinity trkA and low-affinity P75. They concluded that the association rate is indeed diffusion controlled, but that the dissociation rate is not diffusion controlled and is about two orders of magnitude higher for the p75 receptor (reviewed in Meakin and Shooter, 1992). Keino-Masu et al. (1996) measured Hill coefficients for the binding of netrin to the DCC receptor in the range 1.2–1.5. This indicates a small amount of pos-

itive cooperativity; i.e., the binding of each ligand molecule facilitates the binding of the next ligand molecule, whereas the model assumes these events are completely independent. Ephrin molecules may not be internalized by Eph-expressing growth cones, but instead may be bound and then released, violating the internalization assumption used for calculating the flux; ligand multimerization is required for receptor phosphorylation, violating the simple signal to noise criterion; and the time scale of activation of Eph receptors can be of the order of 30 min or more, perhaps owing to a requirement for multimeric aggregation of receptors, violating the assumption that the growth cone responds to the equilibrium fraction of bound receptors (reviewed in Gale and Yancopoulous (1997)). However, despite these apparent limitations on the applicability of the model, it still produces quantitative values in reasonable agreement with experimental measurements. Work following Berg and Purcell has attempted to relax some of the assumptions described above (e.g., DeLisi, 1981; DeLisi et al., 1982; DeLisi and Marchetti, 1983), and these models may be more appropriate for describing gradient sensing in the cases just described. However, these more complex models necessarily involve many parameters which have not yet been measured for growth cones. For instance, DeLisi et al. (1982) analyzed the relative efficiency of spatial versus temporal sensing mechanisms in a model which does not assume the reaction is diffusion limited. In this case, the formuli for $\Delta C/C$ depend in a subtle way on several reaction rate constants rather than just the diffusion constant in the diffusion limited case.

Another limitation of the Berg and Purcell model is that it makes an incorrect prediction about gradient sensitivity should vary with absolute concentration. Equation (3) says that the minimum detectable gradient steepness should tend to a small constant value as the concentration becomes large. In effect, the assumption is that as long as the signal-to-noise criterion is satisfied a gradient can be detected, even if this corresponds to a difference in binding between the two sides of the sensing device of less than one receptor. In reality, it is well documented for leukocytes (e.g., Zigmond (1981)), and it seems reasonable to infer from sparse data for growth cones that the minimum detectable gradient steepness is smallest at a concentration of K_D, and increases as the concentration rises above K_D so that at concentrations of 10 or 100 K_D, a gradient of any size is no longer detectable. This behavior is captured in the alternative model of Lauffenburger (1982), which assumes that gradient detection is always possible provided that a certain threshold difference in the number of receptors bound on the two sides of the sensing device is exceeded. At concentrations much higher than K_D, the signal to noise ratio is large, but nearly all the receptors are bound so that the absolute difference in binding between the two sides of the growth cone is small. A direction for future work is to derive the implications of this model for growth cone sensing; however, again it relies on parameters such as reaction rates that have yet to be measured.

To make progress in the quantitative understanding of the mechanisms of axonal gradient detection, it is thus necessary to measure the concentration of ligand in terms of molecules per unit volume in three-dimensional cases and molecules per unit area in two-dimensional cases *in vivo* and *in vitro*, the number of appropriate receptors on growth cones, and the full set of reaction rate constants for receptor–ligand interactions such as netrin/DCC and the ephrin/Eph family. It is also necessary to make more systematic measurements, as have been done for leukocytes and bacteria, of the minimum detectable gradient, and how this varies with concentration. This will allow competing theories of axonal gradient detection to be directly compared.

The authors thank Linda Richards, David Litwack, and Rob Cassidy for helpful comments on an earlier version of the manuscript. This work was partly supported by DOD Grant DAMD17-93-V-3018.

REFERENCES

Adler J. 1975. Chemotaxis in bacteria. Annu Rev Biochem 44:341–356.

Alt W. 1980. Biased random walk models for chemotaxis and related diffusion approximations. J Math Biol 9:147–177.

Baier H, Bonhoeffer F. 1992. Axon guidance by gradients of a target-derived component. Science 255:472–475.

Berg HC. 1975. Chemotaxis in bacteria. Annu Rev Biophys Bioeng 4:119–136.

Berg HC. 1993. Random walks in biology. Princeton, NJ: Princeton University Press.

Berg HC, Purcell EM. 1977. Physics of chemoreception. Biophys J 20:193–219.

Cheng HJ, Nakamoto M, Bergemann AD, Flanagan JG. 1995. Complementary gradients in expression and binding of Elf-1 and Mek4 in development of the topographic retinotectal projection map. Cell 82:371–381.

Colamarino SA, Tessier-Lavigne M. 1995. The axonal chemoattractant netrin-1 is also a chemorepellent for trochlear motor axons. Cell 81:621–629.

Dahlquist FW, Lovely P, Koshland DE. 1972. Quantitative analysis of bacterial migration in chemotaxis. Nat N Biol 236:120–123.

Deiner MS, Kennedy TE, Fazeli A, Serafini T, Tessier-

Lavigne M, Sretavan DW. 1997. Netrin-1 and DCC mediate axon guidance locally at the optic disc: loss of function leads to optic nerve hypoplasia. Neuron 19:575–589.

de la Torre JR, Höpker VH, Ming G-L, Poo M-M. 1997. Turning of retinal growth cones in a netrin-1 gradient mediated by the netrin receptor DCC. Neuron 19:1211–1224.

DeLisi C. 1981. The magnitude of signal amplification by ligand-induced receptor clustering. Nature 289:322–323.

DeLisi C, Marchetti F. 1983. A theory of measurement error and its implications for spatial and temporal gradient sensing during chemotaxis II. The effects of non-equilibriated receptor binding. Cell Biophys 5:237–253.

DeLisi C, Marchetti F, Del Grosso G. 1982. A theory of measurement error and its implications for spatial and temporal gradient sensing during chemotaxis. Cell Biophys 4:211–229.

Devreotes PN, Zigmond SH. 1988. Chemotaxis in eukaryotic cells: a focus on leukocytes and *Dictyostelium.* Annu Rev Cell Biol 4:649–686.

Drescher U, Kremoser C, Handwerker C, Loschinger J, Noda M, Bonhoeffer F. 1995. In-vitro guidance of retinal ganglion-cell axons by RAGS, a 25 KDa tectal protein related to ligands for Eph receptor tyrosine kinases. Cell 82:359–370.

Eisenbach M. 1996. Control of bacterial chemotaxis. Mol Microbiol 20:903–910.

Flanagan JG, Vanderhaeghen P. 1998. The ephrins and Eph receptors in neural development. Annu Rev Neurosci 21:309–345.

Ford RM. 1992. Mathematical modeling and quantitative characterization of bacterial motility and chemotaxis. In: Hurst CJ, editor. Modeling the metabolic and physiology activities of microorganisms. New York: Wiley. p 177–215.

Friedman GC, O'Leary DDM. 1996. Eph receptor tyrosine kinases and their ligands in neural development. Curr Opin Neurobiol 6:127–133.

Gale NW, Holland SJ, Valenzuela DM, Flenniken A, Pan L, Ryan TE, Henkemeyer M, Strebhardt K, Hirai H, Wilkinson DG, Pawson T, Davis S, Yancopouos GD. 1996. Eph receptors and ligands comprise 2 major specificity subclasses and are reciprocally compartmentalized during embryogenesis. Neuron 17:9–19.

Gale NW, Yancopoulos GD. 1997. Ephrins and their receptors: a repulsive topic? Cell Tissue Res 290:227–241.

Gao PP, Zhang JH, Yokoyama M, Racey B, Dreyfus CF, Black IB, Zhou R. 1996. Regulation of topographic projection in the brain: Elf-1 in the hippocampalseptal system. Proc Natl Acad Sci USA 93:11161–11166.

Goodhill GJ. 1997. Diffusion in axon guidance. Eur J Neurosci 9:1414–1421.

Goodhill GJ. 1998. Mathematical guidance for axons. Trends Neurosci 21:226–231.

Goodhill GJ, Baier H. 1998. Axon guidance: stretching gradients to the limit. Neural Comput 10:521–527.

Goodman CS. 1996. Mechanisms and molecules that control growth cone guidance. Annu Rev Neurosci 19:341–377.

Halfter W. 1996. The behavior of optic axons on substrate gradients of retinal basal lamina proteins and merosin. J Neurosci 16:4389–4401.

Heffner CD, Lumsden AGS, O'Leary DDM. 1990. Target control of collateral extension and directional growth in the mammalian brain. Science 247:217–220.

Keino-Masu K, Masu M, Hinck L, Leonardo ED, Chan SS-Y, Culotti JG, Tessier-Lavigne M. 1996. *Deleted in Colorectal Cancer (DCC)* encodes a netrin receptor. Cell 87:175–185.

Kennedy TE, Tessier-Lavigne M. 1995. Guidance and induction of branch formation in developing axons by target-derived diffusible factors. Curr Opin Neurobiol 5:83–90.

Kennedy TE, Serafini T, de al Torre JR, Tessier-Lavigne M. 1994. Netrins are diffusible chemotropic factors for commissural axons in the embryonic spinal cord. Cell 78: 425–435.

Keynes R, Cook GMW. 1995. Axon guidance molecules. Cell 83:161–169.

Keynes R, Tannahill D, Morgenstern DA, Johnson AR, Cook GMW, Pini A. 1997. Surround repulsion of spinal sensory axons in higher vertebrate embryos. Neuron 18: 889–897.

Lauffenburger DA. 1982. Influence of external concentration fluctuations on leukocyte chemotactic orientation. Cell Biophys 4:177–209.

Lauffenburger DA, Tranquillo RT, Zigmond SH. 1988. Concentration gradients of chemotactic factors in chemotaxis assays. Methods Enzymol 162:85–101.

Lohof AM, Quillan M, Dan Y, Poo M-M. 1992. Asymmetric modulation of cytosolic cAMP activity induces growth cone turning. J Neurosci 12:1253–1261.

Lumsden AGS, Davies AM. 1983. Earliest sensory nerve fibres are guided to peripheral targets by attractants other than nerve growth factor. Nature 306:786–788.

Lumsden AGS, Davies AM. 1986. Chemotropic effect of specific target epithelium in the developing mammalian nervous system. Nature 323:538–539.

MacLennan AJ, McLaurin DL, Marks L, Vinson EN, Pfeifer M, Szulc SV, Heaton MB, Lee N. 1997. Immunohistochemical localization of netrin-1 in the embryonic chick nervous system. J Neurosci 17:5466–5479.

Macnab RM, Koshland DE. 1972. The gradient-sensing mechanism in bacterial chemotaxis. Proc Natl Acad Sci USA 69:2509–2512.

Manson MD. 1992. Bacterial motility and chemotaxis. Adv Microbial Physiol 33:277–346.

Mason CA, Wang LC. 1997. Growth cone form is behavior-specific and, consequently, position-specific along the retinal axon pathway. J Neurosci 17:1086–1100.

McCloskey MA, Poo M-M. 1986. Rates of membrane-associated reactions—reduction of dimensionality revisited. J Cell Biol 102:88–96.

Meakin SO, Shooter EM. 1992. The nerve growth family of receptors. Trends Neurosci 15:323–331.

Ming G-L, Song H-J, Berninger B, Holt CE, Tessier-Lavigne M, Poo M-M. 1997. cAMP-dependent growth cone guidance by netrin-1. Neuron 19:1225–1235.

Monschau B, Kremoser C, Ohta K, Tanaka H, Kaneko T, Yamada T, Handwerker C, Hornbereger MR, Löschinger J, Pasquale EB, Siever DA, Verderame MF, Müller B, Bonhoeffer F, Drescher U. 1997. Shared and distinct functions of RAGS and ELF-1 in guiding retinal axons. EMBO J 16:1258–1267.

Myers PZ, Bastiani MJ. 1993. Growth cone dynamics during the migration of an identified commissural growth cone. J Neurosci 13:127–143.

O'Leary DDM, Yates PA, McLaughlin T. 1999. Molecular development of sensory maps: representing sights and smells in the brain. Cell 96:255–269.

Pini A. 1993. Chemorepulsion of axons in the developing mammalian central nervous system. Science 261:95–98.

Placzek M, Tessier-Lavigne T, Yamada T, Dodd J, Jessell TM. 1990. Guidance of developing axons by diffusible chemoattractants. Cold Spring Harbor Symp Quant Biol 55:279–289.

Poo M-M. 1982. Rapid lateral diffusion of functional ACh receptors in embryonic muscle cell membrane. Nature 295:332–334.

Rehder V, Kater SB. 1996. Filopodia on neuronal growth cones: multi-functional structures with sensory and motor capabilities. Semin Neurosci 8:81–88.

Richards LJ, Koester SE, Tuttle R, O'Leary DDM. 1997. Directed growth of early cortical axons is influenced by a chemoattractant released from an intermediate target. J Neurosci 17:2445–2458.

Rosentreter SM, Davenport RW, Löschinger J, Huf J, Jung J, Bonhoeffer F. 1998. Response of retinal ganglion cell axons to striped linear gradients of repellent guidance molecules. J Neurobiol 37:541–562.

Segel LA. 1977. A theoretical study of receptor mechanisms in bacterial chemotaxis. SIAM J Appl Math 32:653–665.

Serafini T, Kennedy TE, Galko MJ, Mirzayan C, Jessell TM, Tessier-Lavigne M. 1994. The netrins define a family of axon outgrowth-promoting proteins homologous to *C. elegans* UNC-6. Cell 78:409–424.

Serafini T, Colamarino SA, Leonardo ED, Wang H, Beddington R, Skarnes WC, Tessier-Lavigne M. 1996. Netrin-1 is required for commissural axon guidance in the developing vertebrate nervous system. Cell 87:1001–1014.

Shirasaki R, Katsumata R, Murakami F. 1998. Change in chemoattractant responsiveness of developing axons at an intermediate target. Science 279:105–107.

Song H-J, Ming G-L, Poo M-M. 1997. cAMP-induced switching in turning direction of nerve growth cones. Nature 388:275–279.

Stoeckli ET, Sonderegger P, Pollerberg GE, Landmesser LT. 1997. Interference with axonin-1 and NrCAM interactions unmasks a floor-plate activity inhibitory for commissural axons. Neuron 18:209–221.

Sutter A, Riopelle RJ, Harris-Warwick RM, Shooter EM. 1979. Nerve growth factor receptors. J Biol Chem 254: 5972–5982.

Tanaka E, Sabry J. 1995. Making the connection: cytoskeletal rearrangements during growth cone guidance. Cell 83:171–176.

Tessier-Lavigne M. 1995. Eph receptor tyrosine kinases, axon repulsion, and the development of topographic maps. Cell 82:345–348.

Tessier-Lavigne M, Goodman CS. 1996. The molecular biology of axon guidance. Science 274:1123–1133.

Tessier-Lavigne M, Placzek M. 1991. Target attraction—are developing axons guided by chemotropism? Trends Neurosci 14:303–310.

Tessier-Lavigne M, Placzek M, Lumsden AGS, Dodd J, Jessell TM. 1988. Chemotropic guidance of developing axons in the mammalian central nervous system. Nature 336:775–778.

Tranquillo RT. 1990. Theories and models of gradient perception. In: Armitage J, Lackie JM, editors. Biology of the chemotactic response. Cambridge: Cambridge University Press. p 35–75.

Tranquillo RT, Lauffenburger DA. 1986. Consequences of chemosensory phenomena for leukocyte orientation. Cell Biophys 8:1–46.

Tranquillo RT, Lauffenburger DA. 1987. Stochastic-model of leukocyte chemosensory movement. J Math Biol 25: 229–262.

Wiegel FW. 1983. Diffusion and the physics of chemoreception. Phys Rep 95:283–319.

Zheng JG, Felder M, Conner JA, Poo M-M. 1994. Turning of growth cones induced by neurotransmitters. Nature 368:140–144.

Zheng JG, Wan J-J, Poo M-M. 1996. Essential role of filopodia in chemotropic turning of nerve growth cone induced by a glutamate gradient. J Neurosci 16:1140–1149.

Zigmond SH. 1974. Mechanisms of sensing chemical gradients by polymorphonuclear leukocytes. Nature 249: 450–452.

Zigmond SH. 1977. Ability of polymorphonuclear leukocytes to orient in gradients of chemotactic factors. J Cell Biol 75:606–616.

Zigmond SH. 1981. Consequences of chemotactic peptide receptor modulation for leukocyte orientation. J Cell Biol 88:644–647.